ELSEVIER

Nuclear Instruments and Methods in Physics Research A 378 (1996) 149-154

NUCLEAR INSTRUMENTS & METHODS IN PHYSICS RESEARCH Section A

A fast position sensitive microchannel plate detector for ray-tracing of charged particles

O.H. Odland [a], W. Mittig [a,*], A. Lépine-Szily [a,b], G. Fremont [a], M. Chartier [a], M. MacCormick [a], J.M. Casandjian [a]

[a] GANIL, Grand Accélérateur National d'Ions Lourds, National Heavy Ion Laboratory, B.P. 5027, 14021 Caen Cedex, France
[b] IFUSP-Universidade de São Paulo, C.P. 20516, 14098, São Paulo, Brazil

Received 9 January 1996; revised form received 12 April 1996

Abstract

Studies of nuclear reactions by the use of secondary beams involve the need of ray-tracing of either the incident beam or the reaction products. For high resolution experiments, the material interposed to the trajectory of particles must be very thin, in order to produce a minimum of perturbation of their characteristics. Secondary electrons emitted from thin foils are well suited for fast position determination. A microchannel plate detector has been developed in order to accomplish the tracing of these electrons. A parallel ***E***- and ***B***-field configuration, applied as a focusing device for the emitted electrons, produces an image of a reaction vertex. Thus an image of the trajectory of particles can be obtained by placing the electron producing foil into the beamline and record the position of the accelerated and focused electrons hitting a grid of sensewires.

1. Introduction

1.1. Objectives

For many experiments involving charged particles, it is necessary to determine their trajectory before and/or after a reaction target. Experiments using secondary beams and reactions induced by these in a target will benefit from information about the position in space and time of the incident beam of particles. At least secondary beams produced by fragmentation will have a very bad beam quality, this is, a large emittance ε. The influence of this on the quality of the final results can be avoided if we measure, particle by particle, the coordinates in the horizontal and the vertical plane. With a position resolution of 0.5 mm and with two detectors 1 m apart, this results in an emittance of $\varepsilon = 0.25\pi$ mm $\times$ 0.5 msr $\approx 0.1\pi$ mm mrad, which is an excellent effective emittance, if the straggling introduced by the detector is small. The same information may be wanted for the reaction products.

If particle-ray tracing is done with a high resolution detector, it is essential that the perturbation is held at a minimum level. The ray-tracing may in general be done with different kinds of detectors:

- Drift chambers, with a gas-filled active area. Electrons created by ionizing radiation within the detector are caused to drift towards a collecting grid of sensewires.
- Parallel plate avalanche detectors, particularly useful in applications involving heavy charged particles where the associated radiation damage in solid-state detectors may prohibit their use.
- Silicon detectors, which however are too thick for the present application.

In the situation considered here, the detector has to be thin, $\sim$ 50–100 μg/cm^2, and the tracing process has to be fast, since the particle characteristics are to be used as references for the electronics in the experimental setup. There is a need for a detector with a high count rate capacity.

These guidelines lead to a microchannel plate detector with imaging capabilities [1–5].

1.2. Optics, general description

The ions, whose positions are to be detected, will pass through a very thin foil, where the creation of secondary electrons will take place. The foil we used mostly are 0.5 μm mylar foils with 20 μg/cm^2 Al evaporated on one face for electrical conductivity. The number of secondary electrons is enhanced by a factor of $\sim$ 5 by a thin ($\sim$ 500 Å) CsI coating on the Al [6,7].

The secondary electrons are accelerated towards the microchannel plate detector, which is placed outside of the trajectory of particles in order not to intercept them, see Fig. 1. The number of electrons are amplified by two microchannel

* Corresponding author. Tel. +33 31 45 46 47, e-mail mittig@ganac4.in2p3.fr.

PII S0168-9002(96)00441-X

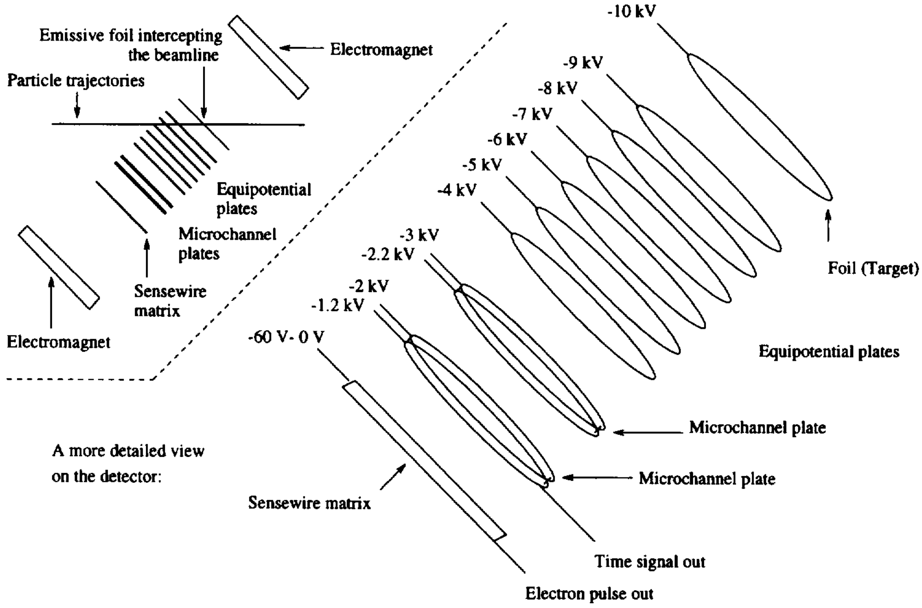

Fig. 1. A schematic diagram of the microchannel plate detector developed for fast ray-tracing of secondary electrons. Only the emissive foil perturbs the particle trajectories in the beamline. Upper left; schematic device, lower right; electron guidance, multiplication and position readout schematics.

plates with an amplification of the order of 10^6 times the incoming number of electrons, and transferred to a position readout device. The microchannel plates have a diameter of 70 mm and the sensewire matrix is 65×65 mm^2.

When using microchannel plates as we do here one must devise a method of reading out the signals from such rather large channel plates while maintaining high spatial resolution, small deadtime and, if possible, little or no distortion, and negligible cross-correlation between x- and y- coordinates [8]. In addition, the counting-rate limitations must be taken into account; i.e. the desired spatial resolution must be obtained with the smallest possible microchannel plate gain since the maximum microchannel plate count rate decreases linearly with microchannel plate modal gain.

The best chance of satisfying all of these requirements appears to be with delay line readout. With such a readout, output signal levels do not depend on electrode capacitances, which increase as the readout size increases. High quality delay lines are simple to construct and can be designed for high counting rates.

In order to obtain a time reference signal for the electronics, a "fast" time signal is extracted from the output side of the second microchannel plate. The pulse signal is taken out after a capacitor (1 nF) and is thereafter used as a reference time signal ("start" signal) for the later, delayed, pulses from the sensewire grid ("stop" signals).

The readout consists of two delaylines, sensewires, on which the output charge from the second microchannel plate is collected. The delayline consists of flattened bifilar helices, which are similar to parallel wire transmission lines (differential cables), see Fig. 2.

These bifilar helices are, as shown in Fig. 2, wrapped around a printed circuit board. With respect to Ref. [8] the technology of this is considerably changed; gold plated tungsten wires of 150 μm are used instead of copper wires, rounded frames are used instead of rectangular ones, and grounding plates are mounted around the edges of the matrix in order to reduce possible reflections due to mismatch of characteristic resistances.

We connected the two adjacent ends of a parallel pair to the two inputs of a low noise differential amplifier, using one amplifier at each end of a delayline. By suitable adjust-

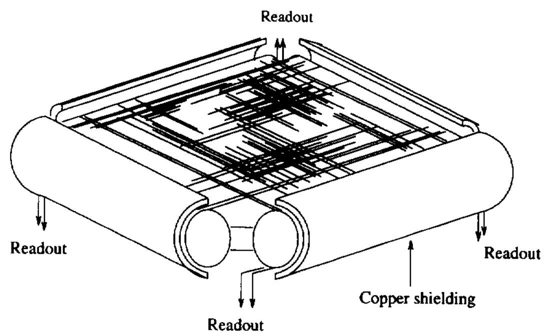

Fig. 2. The delay line sensewire matrix. The matrix consists of parallel coupled wires in the x- and y-direction, one collecting and one non-collecting, both have a length corresponding to 20 ns. The spacing between the wires is 0.5 mm. The signal pulse is read out in both ends of each pair of wires. A copper shielding is merged around the rounded frames in order to avoid possible signal reflections due to mismatch of the characteristic resistance.

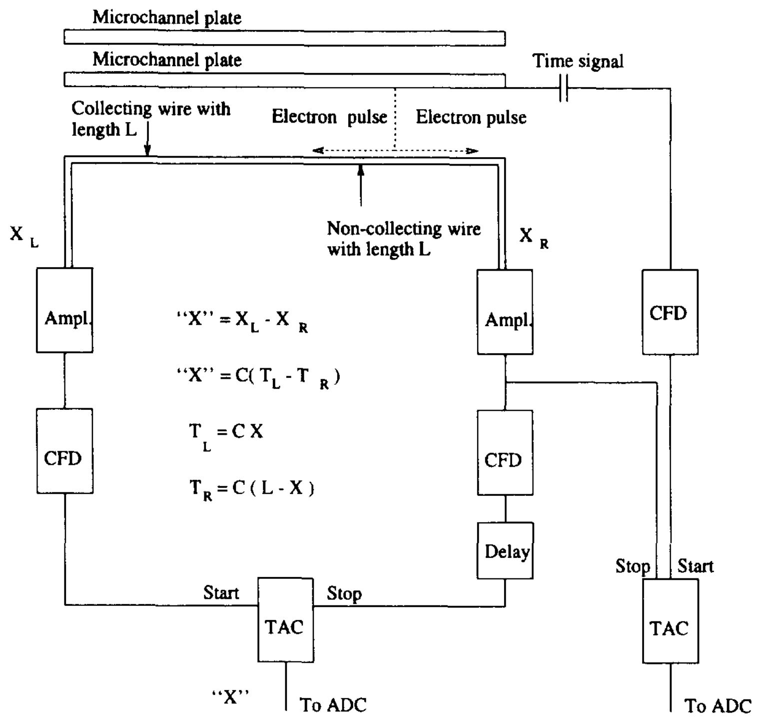

Fig. 3. A schematic view of the principle of position determination by the use of delay lines. The signal pulse arriving on the wires is read out in both ends of the parallel pair. The figure shows only the x-position part of the sensewire couplings, a similar setup is applied for the y-position determination.

ment of dc-voltages on the delaylines, half of the charge is collected on each delay line, in the x- and y-direction, and on each delay line the charge is collected on only one wire of the parallel pair.

Due to the differential amplifier, the final signal is not influenced by capacitive coupling, it corresponds only to the collected charge signal. Without this differential effect, prepulses are produced, with an amplitude of the same size as the real signals.

The outputs of the differential amplifiers are fed to constant fraction timing discriminators (CFD) in order to make measurements of the difference in arrival times of the pulses from the two ends of each delay line.

We have further used Time-to-Amplitude-Converters (TAC) and Analog-to-Digital-Converters (ADC) before the signals arrived in VME-crates.

The whole setup assembly is placed inside a vacuum tube.

The delay line matrix has a characteristic resistance of 200 Ω. In order to be able to transmit the signals from the matrix by standard 50 Ω cables to standard fast electronics, pulse transformers (200–50 Ω) were used at the end of the wires from the matrix.

The electrons emerging from the microchannel plates induce an electric pulse on the grid of sensewires. When electrons hit a wire, the distance from the hit to both ends of the wire is measured, see Fig. 3. When the sum of the time it takes for the pulse to travel to both sides is measured, it will for real pulses give the total time it takes to travel the full length of the wire. This may be used for background- and pile-up rejection.

The best efficiency of microchannels for electrons is in the energy range between 200–500 eV [9]. The better choice is therefore to use a quite low (100–400 V) acceleration potential in order to achieve a high detection efficiency for low-ionizing particles.

The secondary electrons have some initial energy, this is of the order of 1 eV [10]. This will decorrelate the electron's impact on the foil and therefore blur the image of these on the microchannel plate device. A simple estimate shows, that in terms of ion optics, the emittance is of the order of; $\varepsilon = 70/2\pi \times 50$ msr $= 3500\pi$ mm mrad.

This is why we developed a focussing device between the foil and the microchannel plates, where we use a magnetic field parallel with the accelerating electric field as described below, probably the only way to handle such an enormous emittance.

1.3. General formulae for the optics

In the presence of a magnetic field, $\boldsymbol{B}$, and an electric field, $\boldsymbol{E}$, the forces acting on an electrical charged particle will be given by

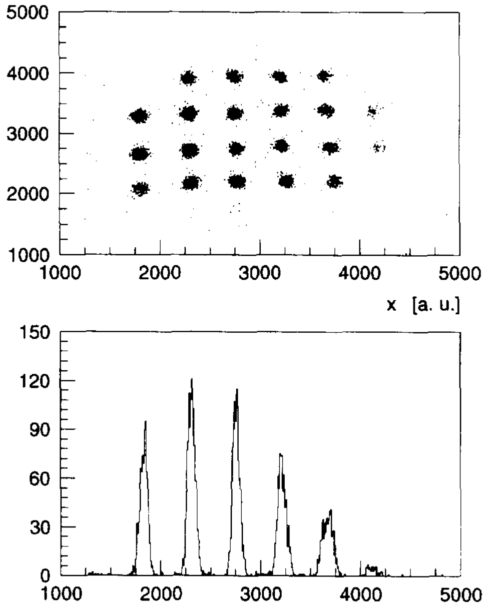

Fig. 4. The grid pattern (top) shows the image of α-particles illuminating a slotted plate which was placed in front of the secondary electrons emission foil. The electrons recorded were in coincidence with α-particles hitting a silicon detector. The distance between the centers of the holes in the plate is 5 mm, the diameter of the holes is 1 mm. The peaks (bottom) are a projection of the grid pattern onto the x-axis.

$$\boldsymbol{F} = q\boldsymbol{E} + q\boldsymbol{v} \times \boldsymbol{B}. \tag{1}$$

We can decompose the particle velocity,

$$\boldsymbol{v} = \boldsymbol{v}_{\perp} + \boldsymbol{v}_{\parallel}, \tag{2}$$

where we consider $\boldsymbol{v}_{\parallel}$ to be the electron's velocity parallel to the $\boldsymbol{E}$-field direction, and $\boldsymbol{v}_{\perp}$ to be the electron's velocity in the direction perpendicular to the $\boldsymbol{E}$-field direction. Here we consider the application of this detector in the case where the $\boldsymbol{E}$- and $\boldsymbol{B}$-fields are parallel. In this case, the electrons have a constant velocity in the perpendicular direction, $|\boldsymbol{v}_{\perp}|$ = constant, and the electrons are moving in circular trajectories in the plane perpendicular to the $\boldsymbol{E}$- and $\boldsymbol{B}$-fields with the cyclotron frequency given by

$$\omega_c = (qB)/(\gamma m), \tag{3}$$

where ω_c is the cyclotron frequency, and the radius of the orbital motion of the electrons is given by

$$r = (mv)/(qB) \tag{4}$$

in a non-relativistic approximation.

We can also decompose the initial energy of the secondary electrons, where the components are

$$E_0 = E_{0\parallel} + E_{0\perp}, \tag{5}$$

$$E_0 = \tfrac{1}{2}m(v_{0\parallel}^2 + v_{0\perp}^2). \tag{6}$$

Now, the typical initial energy of the secondary electrons is low ($\sim$ 1 eV) compared to the acceleration energy

$$eV_{acc} \gg E_{0\parallel}, \tag{7}$$

i.e. that the electrons initial energy, no matter how it is spread, is small compared to the accelerating field and, in our assumption, can thus be neglected. This implies that the transit time, t_{tr}, for the secondary electrons, the time for the electrons to traverse from the foil, through the acceleration gap and through the microchannel plates, to the grid of sensewires, is essentially a constant for the given distance between the foil and the grid. By neglecting the initial velocity, $\boldsymbol{v}_{0\parallel} \ll \boldsymbol{v}_{\parallel}$, we have

$$t_{tr} = \sqrt{(2md)/(qV_{acc})} = 3375\sqrt{d/V_{acc}} \quad [\text{ns}], \tag{8}$$

where d is the distance, [m], between the emissive foil and the grid of sensewires.

It can be shown that the equation of motion for the electrons in the acceleration gap is given as

$$\rho(B,t) = \left\{ \left(\frac{mv_{\perp}}{qB}\right)^2 \left[\left(\cos\left(\frac{Bq}{m}\sqrt{\frac{2md}{qV_{acc}}}\right) - 1 \right)^2 + \left(\sin\left(\frac{Bq}{m}\sqrt{\frac{2md}{qV_{acc}}}\right)\right)^2 \right] \right\}^{1/2}, \tag{9}$$

where $\rho(B,t)$ is defined as the deviation from a straight line in the z-direction seen in the x–y plane, i.e., the difference between the impact position on the microchannel plates and the position of a projection of the origin of a secondary electron.

We deduce from this, that for

$$\frac{Bq}{m}\sqrt{\frac{2md}{qV_{acc}}} = n\pi \rightarrow \rho(B,t) = 0 \quad \text{when } n = 2,4,6,8,..., \tag{10}$$

when n is an integer *even* number, i.e., a "perfect" image of the foil is obtained when the secondary electrons have made an integer even number of turns at their cyclotron frequency when they hit the sensewire grid.

According to this we expect to find some optimal field configurations at which the detector gives an as good as possible image of the foil.

2. Description of the device testing

The main issue of the measurements is to obtain a qualitative understanding and a quantitative measure of the detector's resolution capabilities. This is obtained by a series of measurements in which the only variables were the electric- and the magnetic fields.

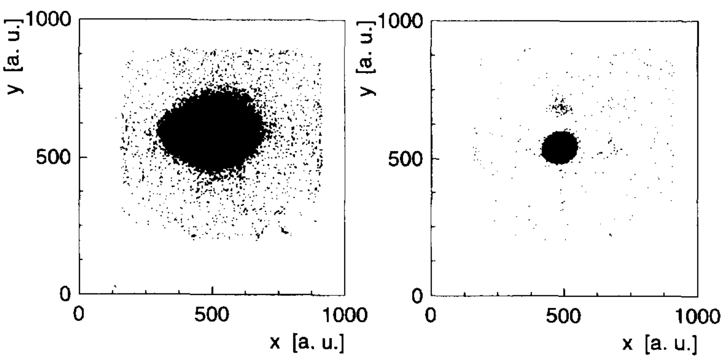

Fig. 5. The image of an α-source with a diameter of 7 mm. This source was used as an emitter of secondary electrons. Left; the sensewire matrix from a run with the applied fields; $E = 4000$ V/m without the magnetic field. Right; the sensewire matrix from a run with the applied field; $E = 4000$ V/m and $B = 3.0$ mT.

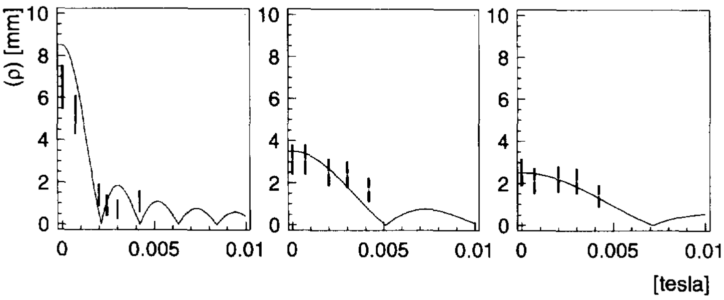

Fig. 6. The measured detector resolution ρ (FWHM) plotted together with the theoretical curve for the resolution function, both plotted as a function of the magnetic field. The plots show the measured resolution for the target voltages 3 kV (left), 5 kV (center) and 7 kV (right), which implies the respective electric fields of 4000-, 24000- and 44000 V/m.

In operative mode, the detector will enable a ray-tracing of secondary electrons emitted from a foil. In the present test we used an emissive foil together with an α-source as particle emitter.

It is further possible to obtain a measurement of the electronics's intrinsic resolution ability. This resolving power can be studied from plots which show the "edges" of the delay line matrix. The sharpness of the edge shows that the intrinsic electronic resolution is ≥ 0.2 mm (FWHM). The time resolution of the electronics is of the order of $\sim$ 200-300 ps (FWHM).

The dimensions of the detector were limited to a minimum in order to be compatible with the dimensions of the Standard DN160 connections used at GANIL. The detector may be mounted on such a connector and be taken in and out of the beamline during experiments.

The magnetic field is set up on electromagnets providing a maximum field of 4.2 mT.

3. Results

In a first test, α-particles emitted from an α-source induced the emission of secondary electrons from the foil and the α-particles hitting a silicon detector are used as a coincidence condition. In Fig. 4 are two plots shown. In both of them we can see a grid pattern which stems from the fact that a slotted plate was placed between the α-source and the secondary electron emission foil.

The distance between the centers of the holes is 5 mm and the diameter of the holes is 1 mm.

In the second test, the results give information about the detectors resolution capability. Here we use secondary electrons emitted directly from the α-source, which now replaced the emissive foil. In Fig. 5 are shown two plots from this test. This geometry provides a much higher counting rate than the preceding one, and was therefore used below.

Both the electric- and the magnetic field are governing the resolution of the detector.

Without the presence of a magnetic field, the emitted particles give a less focused image of the beam spot. The trajectories of the emitted electrons show the momentum dispersion at the moment of the emission, which is maintained by conservation of energy and momentum, will thus tend to spread out the beam spot image.

Under the influence of a magnetic field, the helicoidal movement of the emitted and accelerated particles gives a focussing effect, as apparent from Eqs. (9) and (10).

In Fig. 6 we have plotted the measured detector resolution (FWHM) together with the theoretical curve, given in Eq. (10). We have assumed that the secondary electrons have an initial energy of $\sim$ 1 eV, i.e., a velocity $v_{\perp}$ =

5×10^{-2} cm/ns, and that the transit time for the electrons is constant throughout the potential gap. We have not made any corrections for inhomogeneities in the electric- and the magnetic field.

The magnetic field was measured by a standard probe, the measurements are repeated several times and the field values are given as an average value of these. The error bars of the measured resolution values (FWHM) are assumed to be $\pm 10\%$ of the measured value and also ± 5 channels in the electronic readout from the signals from the sensewire matrix. We have in the plots omitted the error bars for the measurements of the magnetic field, which are small (of the order of some % of the measured values), due to repeated measurements of the fields.

The plots in Fig. 6 also indicate that the resolution decreases as the magnetic field is increased. Further it is apparent that the resolution improves for increasing accelerating voltage.

The optimal resolution was measured with the applied field configuration; $E = 4000$ V/m, $B = 3.0$ mT. The measured minimum resolution value, 0.7 mm (FWHM), have some offset from the theoretical curve, which shows minima at $B = 2.1$ mT and $B = 4.2$ mT. It can be concluded that there is a semiquantitative agreement between the experimental resolution and the theoretical curves.

4. Conclusions

We have developed and tested a microchannel plate detector with delay line readout of position determination for charged particles with the use of ray-tracing of secondary electrons. It is shown that a parallel E- and B-field configuration significantly improves the detector's resolution.

The optimal detector resolution is measured with the electrical field $E = 4 \times 10^3$ V/m and the magnetic field $B = 2.4$ mT.

The tests have shown that a microchannel plate detector like this have a near 100% detection efficiency for the detection of fast particles ($E \geq 50$ MeV/nucleon) with $Z \geq 8$.

Two detectors of this type were constructed and are routinely used in experiments at GANIL.

References

[1] Proc. 2nd London Conf. on Position-Sensitive Detectors, Nucl. Instr. and Meth. A 310 (1991) Nos. 1 and 2.
[2] Proc. 3rd London Conf. on Position-Sensitive Detectors, Nucl. Instr. and Meth. A 348 (1994) Nos. 2 and 3.
[3] E.C. Polacco et al, Nucl. Instr. and Meth. 225 (1984) 5.
[4] J.L. Culhane, Nucl. Instr. and Meth. A 310 (1991) 1.
[5] O.H.W. Siegmund, M. Lampton, R. Raffant and W. Merrick, Nucl. Instr. and Meth. A 310 (1991) 311.
[6] C. Chianelli, P. Ageron, J.P. Bouvet, M. Karolak, S. Martin and J.P. Robert, Nucl. Instr. and Meth. A 273 (1988) 245.
[7] H.L. Siefert et al, Nucl. Instr. and Meth. A 292 (1990) 533.
[8] S.E. Sobottka and M.B. Williams, IEEE Trans. Nucl. Sci. NS-35(1) (1988) 348.
[9] G.W. Fraser, Nucl. Instr. and Meth. 206 (1983) 445.
[10] B.L. Henke et al, J. Appl. Phys. 52 (1981) 1509.